# Optimal $H_\infty$ Control for Linear Periodically Time-Varying Systems in Hard Disk Drives

Jianbin Nie, Richard Conway, *Student Member, IEEE*, and Roberto Horowitz, *Senior Member, IEEE*

***Abstract*—Periodicity frequently occurs in hard disk drives (HDDs) whose servo systems with periodic phenomena can be usually modeled as linear periodically time-varying (LPTV) systems. This paper discusses optimal $H_\infty$ control synthesis for discrete-time LPTV systems via discrete Riccati equations. First, an explicit minimum entropy $H_\infty$ controller for general time-varying systems is obtained. Subsequently, the developed control synthesis algorithm is applied to LPTV systems and it is shown that the resulting controllers are periodic. The proposed control synthesis technique is evaluated through both single and multirate optimal $H_\infty$ track-following control designs. The single-rate servo design shows that our proposed control synthesis technique is more numerically robust in calculating optimal $H_\infty$ controllers for discrete-time linear time-invariant systems than the MATLAB function of "hinfsyn," while the multirate servo design validates its ability of synthesizing multirate controllers to achieve the robust performance of a desired error-rejection function. Moreover, an experimental study—in which the developed control synthesis algorithm on a real HDD with missing position error signal sampling data is implemented—further demonstrates its effectiveness in handling LPTV systems with a large period and attaining desirable disturbance attenuation.**

***Index Terms*—Hard disk drive (HDD), linear periodically time-varying (LPTV) systems, missing position error signal (PES) sample, multirate servos, optimal $H_\infty$ control.**

## I. Introduction

LINEAR periodically time-varying (LPTV) systems are frequently encountered in mechatronic systems [1] including hard disk drives (HDDs), in which the rotation of the disks induces periodic dynamic phenomena. For example, HDD servos with missing position error signal (PES) sampling data have been modeled as LPTV systems according to their natural periodicity related to the disk rotation [2]. Moreover, as illustrated in this paper, HDD servo systems with multirate sampling and actuation [3] can be easily represented as LPTV systems for control synthesis purposes. In this paper, the control design of LPTV systems in HDDs will be considered.

Since there tend to be large variations in HDD dynamics [4] due to variations in manufacture and assembly, the synthesized controller must guarantee the desired level of performance for a large set of HDDs. $H_\infty$ control is a popular control design methodology to make control systems achieve the robust performance criterion that many several HDDs simultaneously satisfy a desired minimum level of error-rejection loop shaping [5]. These techniques are potentially attractive in the design of mass-market mechatronic devices, especially, HDDs, where consistent performance must be attained among tens of thousands of units in a given product line [6]. Furthermore, as shown in this paper, it is useful to extend these optimal $H_\infty$ control design techniques to LPTV systems in HDD servos.

Since the pioneering work of Zames in [7], significant progress has been made in the design of optimal $H_\infty$ control. In [8], a state-space solution to standard $H_\infty$ control problems was given for continuous-time linear time-invariant (LTI) systems. As stated in [9], even though $H_\infty$ control problems for discrete-time LTI systems can be solved by using the well-known bilinear transformation, it is more beneficial to solve the problems directly in the discrete-time domain. In [10], the authors considered $H_\infty$ control synthesis techniques for discrete-time linear time-varying (LTV) systems via the minimum-entropy control paradigm. Using the results and ideas presented in [10], we derive explicit and implementable solutions for optimal $H_\infty$ control of LPTV systems. These solutions via discrete Riccati equations are often more computationally efficient and accurate than the counterpart using semidefinite programs (SDP) [11].

In order to evaluate the effectiveness of the developed optimal $H_\infty$ control synthesis algorithm, we first consider the optimal $H_\infty$ track-following servo design for HDD servo systems with both single and multirate sampling and actuation. The single-rate servo design shows that our proposed control synthesis technique is more numerically robust in calculating optimal $H_\infty$ controllers for discrete-time LTI systems than the MATLAB function "hinfsyn," while the multirate servo design validates its ability of synthesizing multirate controllers to achieve robust performance in terms of a desired error-rejection function. Additionally, an experimental study, carried out on a real disk drive with missing PES sampling data, demonstrates that the proposed control synthesis algorithm is also applicable to LPTV systems with a large period.

This paper is organized as follows. In Section II, we provide preliminary background for the results contained in this paper. In Section III, the optimal $H_\infty$ control synthesis algorithm for LPTV systems is explicitly determined. The developed

Manuscript received March 13, 2011; revised June 14, 2011; accepted August 13, 2011. Date of publication September 29, 2011; date of current version September 12, 2012. Recommended by Technical Editor J. M. Berg. This work was supported by the Computer Mechanics Laboratory, University of California, Berkeley, and by Western Digital Corporation, Irvine, CA.

J. Nie was with the Department of Mechanical Engineering, University of California, Berkeley, CA 94720 USA. He is now with Western Digital Corporation, Irvine, CA 92612 USA (e-mail: njbin.ustc@gmail.com).

R. Conway and R. Horowitz are with the Department of Mechanical Engineering, University of California, Berkeley, CA 94720 USA (e-mail: rconway345@gmail.com; horowitz@berkeley.edu).

Color versions of one or more of the figures in this paper are available online at http://ieeexplore.ieee.org.

Digital Object Identifier 10.1109/TMECH.2011.2166161

1083-4435/$26.00 © 2011 IEEE

control methodology is applied to design $H_\infty$ track-following controllers in Section IV. An experimental study is provided in Section V. Conclusions are given in Section VI.

## II. Preliminaries

Here, we will consider general discrete-time LPTV systems that admit a state-space realization with periodically time-varying entries of the form

$$G \sim \begin{bmatrix} x(k+1) \\ z(k) \\ y(k) \end{bmatrix} = \begin{bmatrix} A(k) & B_1(k) & B_2(k) \\ C_1(k) & D_{11}(k) & D_{12}(k) \\ C_2(k) & D_{21}(k) & 0 \end{bmatrix} \begin{bmatrix} x(k) \\ w(k) \\ u(k) \end{bmatrix} \tag{1}$$

where $w(k)$ and $u(k)$ are respectively the disturbance and control inputs; $y(k)$ is the measurable output that is accessible to the control system; $z(k)$ is "performance monitoring" output that is used in our optimization cost function. All time-varying matrix entries in $G$ are assumed to be periodic with the period $N$, e.g., $A(k) = A(k+N)$.

Throughout this paper, we use the following notations:

$$B(k) = [\, B_1(k) \quad B_2(k)\,],\ D_{1\bullet}(k) = [\, D_{11}(k) \quad D_{12}(k)\,],$$

$$C(k) = \begin{bmatrix} C_1(k) \\ C_2(k) \end{bmatrix},\ D_{\bullet 1}(k) = \begin{bmatrix} D_{11}(k) \\ D_{21}(k) \end{bmatrix}, \text{ and}$$

$$D(k) = \begin{bmatrix} D_{11}(k) & D_{12}(k) \\ D_{21}(k) & 0 \end{bmatrix}.$$

Before providing our developed control algorithm for the LPTV system in (1), we have the following notations and assumptions similar to the counterpart in [10]. The input disturbance $w(k)$ is assumed to belong to $\ell_2$, the set of all square summable sequences. In addition, the $H_\infty$ norm of LTI systems is generalized as the $\ell_2$-induced norm for discrete-time LTV systems. For an LTV system $H$ with input $w$ and output $z$, its $\ell_2$-induced norm is defined as

$$\|H\|_{2\leftarrow 2} = \left( \sup_{\boldsymbol{w} \in \ell_2 \setminus \{0\}} \frac{\sum_{k=0}^{\infty} z^T(k) z(k)}{\sum_{k=0}^{\infty} w^T(k) w(k)} \right)^{1/2}.$$

A bold operator will denote a linear operator corresponding to a time-varying system. For example, if $\boldsymbol{H}$ is the linear operator corresponding the time-varying system $H$, $\boldsymbol{H}$ has the matrix representation

$$\boldsymbol{H} = \begin{bmatrix} \ddots & \vdots & \vdots & \iddots \\ \cdots & H_{0,0} & H_{0,1} & \cdots \\ \cdots & H_{1,0} & H_{1,1} & \cdots \\ \iddots & \vdots & \vdots & \ddots \end{bmatrix}. \tag{2}$$

Suppose now that the LTV system $H$ in (2) satisifies $\|H\|_{2\leftarrow 2} < \gamma$. Then, the self-adjoint operator $\boldsymbol{I} - \gamma^{-2}\boldsymbol{H}^*\boldsymbol{H}$ has the spectral factorization

$$\boldsymbol{I} - \gamma^{-2}\boldsymbol{H}^*\boldsymbol{H} = \boldsymbol{M}^*\boldsymbol{M}$$

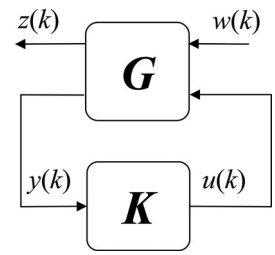


Fig. 1. Block diagram of general LPTV control systems.

where $\boldsymbol{M}$ is a memoryless operator. The entropy of the LTV system $H$ [10] is defined as

$$\boldsymbol{E}(\boldsymbol{H}, \gamma) := -\gamma^2 \text{diag}\left\{ \ln\det(M_{k,k}^T M_{k,k}) \right\}_{k=0}^{\infty}. \tag{3}$$

Given the LPTV system defined in (1), the optimal $H_\infty$ control objective is to find a minimum $\gamma > 0$ and an optimal LTV compensator $K$ with input $y(k)$ and output $u(k)$ so that the $\ell_2$-induced norm of the closed-loop system $\mathcal{F}_\ell(G, K)$ that represents the closed-loop system with the input $w(k)$ and the output $z(k)$ as depicted in Fig. 1 is less than $\gamma$, i.e.

$$\begin{aligned} &\min_{K,\gamma} && \gamma \\ &\text{s.t.} && \|\mathscr{F}_\ell(G, K)\|_{2\leftarrow 2} < \gamma. \end{aligned} \tag{4}$$

## III. $H_\infty$ Control Synthesis for Discrete-Time LPTV Systems

As mentioned in [10], there may exist many controllers that satisfy the inequality in (4) for a given $\gamma$. Using the minimum entropy control framework allows us to choose one particular controller that satisfies the inequality in (4) for given $\gamma$. The usefulness of this framework is that the optimal controller can be synthesized using two Riccati equations. Also, the closed-loop entropy can be used to determine a bound on the closed-loop $H_2$ norm, which means that minimum entropy controllers tend to yield systems with small closed-loop $H_2$ norms. Note that the entropy for a time-varying system in (3) is defined as a memoryless operator. Unlike the minimum entropy for an LTI system, the minimum entropy for an LTV system means that its average entropy is the minimum.

In order to synthesize the optimal $H_\infty$ controller, we first need to check whether or not there exists a controller satisfying the $\ell_2$-induced norm constraint in (4) for each $\gamma$ and, then, utilize a bisection search method to find the minimum $\gamma$ and the corresponding optimal controller. In the minimum entropy control synthesis methodology that follows, for simplicity and without loss of generality, we will assume that $\gamma = 1$.

### A. Minimum Entropy Control for General Discrete-Time LTV Systems

In this section, we will temporarily ignore the periodicity of the LPTV system in (1) and utilize the similar techniques presented in [10] to synthesize the minimum entropy output-feedback control for general LTV systems. In [10], the solution

to the output-feedback control problem is obtained by transforming the output-feedback control problem to an output-estimation control problem and, then, using duality to transform this problem into a disturbance feedforward control problem, which is solved using the solution of a full information control problem. However, no explicit formulas are presented in [10] for controllers synthesized using these steps. Alternatively, this paper synthesizes the output-feedback minimum entropy control for general discrete-time LTV systems in the following three steps.

1) The output feedback control problem is transformed to an output estimation control problem.
2) The output estimation control problem is reduced to the full control problem.
3) The solution to the full control problem is obtained as the dual of the full information control problem, whose solution is provided in [10].

The details of the proposed techniques for the output-feedback control problem reduction is presented in [12]. Utilizing our proposed procedure yields the following unique stabilizing minimum entropy time-varying controller $K$, which satisfies the constraint in (4) and is given by the following state-space realization:

$$\begin{cases} \hat{x}(k+1) = \bar{A}(k)\hat{x}(k) + B_2(k)u(k) + F_t(k)\left(\bar{C}_2(k)\hat{x}(k) \\ \qquad\qquad -y(k)\right) \\ u(k) = -T_{22}^{-1}(k)\bar{C}_{12}(k)\hat{x}(k) + L_t(k)\left(\bar{C}_2(k)\hat{x}(k) - y(k)\right). \end{cases} \tag{5}$$

The parameters used to construct the controller in (5) are updated in the following steps.

1) Solve backward in time, the state-feedback Riccati equation for all $j$:

$$X(j) = A^T(j)X(j+1)A(j) + C_1^T(j)C_1(j) - M(j) \times \left(R(j) + B^T(j)X(j+1)B(j)\right)^{-1} M^T(j) \tag{6}$$

where $M(j) = A^T(j)X(j)B(j) + C_1^T(j)D_{1\bullet}(j)$ and $R(j) = D_{1\bullet}^T(j)D_{1\bullet}(j) - \left[\begin{smallmatrix} I & 0 \\ 0 & 0 \end{smallmatrix}\right]$ so that the solution $X(j)(\succeq 0)$ is bounded for all $j$.

After obtaining the solution $X(j)$ for all $j = 0, 1, 2, \ldots$, we continue to calculate the other parameters.

2) Define $T(k) = \left[\begin{smallmatrix} T_{11}(k) & 0 \\ T_{21}(k) & T_{22}(k) \end{smallmatrix}\right]$ with $T_{11}(k) \succ 0$ and $T_{22}(k) \succ 0$ and compute $T(k)$ using

$$R(k) + B^T(k)X(k+1)B(k) = T^T(k)JT(k) \tag{7}$$

where $R(k) = D_{1\bullet}^T(k)D_{1\bullet}(k) - \left[\begin{smallmatrix} I & 0 \\ 0 & 0 \end{smallmatrix}\right]$, $J = \left[\begin{smallmatrix} -I & 0 \\ 0 & I \end{smallmatrix}\right]$.

3) Get $\left[\begin{smallmatrix} F_1(k) \\ F_2(k) \end{smallmatrix}\right] = (R(k) + B^T(k)X(k+1)B(k))^{-1}M^T(k)$.

4) Calculate the following matrices for the filtering Riccati equation: $\bar{A}(k) = A(k) + B_1(k)F_1(k)$, $\bar{C}_2(k) = C_2(k) + D_{21}(k)F_1(k)$, and $\bar{C}_{12}(k) = -T_{22}(k)F_2(k)$. Let $D_\perp(k)$ be an orthogonal matrix of $D_{12}(k)$. In addition, define a matrix $W$, such that $W^T(k)W(k) = I - T_{11}^T(k)T_{11}(k)$ and $W(k)$ has appropriate dimensions so that the following matrix multiplication is well defined:

$$\begin{bmatrix} \bar{D}_{111}(k) \\ \bar{D}_{112}(k) \end{bmatrix} = D_\perp(k)W(k) + D_{12}(k)T_{21}(k).$$

5) Update forward in time, the filtering Riccati equation solution with zero-initial condition:

$$Y(k) = \bar{A}(k)Y(k-1)\bar{A}^T(k) + B_1(k)B_1^T(k) - \tilde{M}(k) \times \left(\tilde{R}(k) + \begin{bmatrix} \bar{C}_{12}(k) \\ \bar{C}_2(k) \end{bmatrix} Y(k-1) \begin{bmatrix} \bar{C}_{12}(k) \\ \bar{C}_2(k) \end{bmatrix}^T\right)^{-1} \times \tilde{M}^T(k) \tag{8}$$

where $Y(k) \succeq 0$ and

$$\tilde{M}(k) = \bar{A}(k)Y(k-1)\begin{bmatrix} \bar{C}_{12}(k) \\ \bar{C}_2(k) \end{bmatrix}^T + B_1(k)\begin{bmatrix} \bar{D}_{112}(k) \\ D_{21}(k) \end{bmatrix}^T$$

$$\tilde{R}(k) = \begin{bmatrix} \bar{D}_{112}(k) \\ D_{21}(k) \end{bmatrix}\begin{bmatrix} \bar{D}_{112}(k) \\ D_{21}(k) \end{bmatrix}^T - \begin{bmatrix} I & 0 \\ 0 & 0 \end{bmatrix}.$$

6) Define $\tilde{T}(k) = \left[\begin{smallmatrix} \tilde{T}_{11}(k) & \tilde{T}_{12}(k) \\ 0 & \tilde{T}_{22}(k) \end{smallmatrix}\right]$, with $\tilde{T}_{11}(k) \succ 0$ and $\tilde{T}_{22}(k) \succ 0$, and compute $\tilde{T}(k)$ using

$$\tilde{R}(k) + \begin{bmatrix} \bar{C}_{12}(k) \\ \bar{C}_2(k) \end{bmatrix} Y(k-1) \begin{bmatrix} \bar{C}_{12}(k) \\ \bar{C}_2(k) \end{bmatrix}^T = \tilde{T}(k)\tilde{J}\tilde{T}^T(k) \tag{9}$$

where $\tilde{J} = \begin{bmatrix} -I & 0 \\ 0 & I \end{bmatrix}$.

7) Obtain

$$\begin{bmatrix} \tilde{F}_1(k) \\ \tilde{F}_2(k) \end{bmatrix} = \left(\tilde{R}(k) + \begin{bmatrix} \bar{C}_{12}(k) \\ \bar{C}_2(k) \end{bmatrix} Y(k-1) \times \begin{bmatrix} \bar{C}_{12}(k) \\ \bar{C}_2(k) \end{bmatrix}^T\right)^{-1} \tilde{M}^T(k). \tag{10}$$

8) Calculate the filter gains

$$L_t(k) = T_{22}^{-1}(k)\tilde{T}_{12}(k)\tilde{T}_{22}^{-1}(k)$$
$$F_t(k) = \tilde{F}_1^T(k)\tilde{T}_{12}(k)\tilde{T}_{22}^{-1}(k) + \tilde{F}_2^T(k).$$

### B. $H_\infty$ Control Synthesis Algorithm for LPTV Systems

It should be noted that because we are solving an infinite-horizon problem and the state-feedback Riccati equation given in Step 1 must be solved backward in time, there is no methodology for determining the solution in general [10]. Thus, the controller in (5) is not implementable for general time-varying systems. However, it is well known that the bounded stabilizing solutions to the Riccati equations in Step 1 and Step 5 are unique [10]. Moreover, we will show in Lemma 1 that these solutions for LPTV systems are also periodic. As a result, the solutions to two Riccati equations converge to the corresponding stabilizing solutions, which can be solved in a straightforward

manner by iteration, starting, respectively, from zero-final and zero-initial conditions.

*Lemma 1:* For LPTV systems with period $N$, the solutions to the Riccati equations in both Step 1 and Step 5 are periodic with period $N$. Furthermore, the $H_\infty$ controller given by (5) is also periodic with period $N$.

*Proof:* First, we will show the periodicity of the solution to the discrete Riccati equation (6) in Step 1. Suppose $(\ldots, X(j), X(j+1), \ldots)$ is a solution to the discrete Riccati equation in (6), which means that

$$X(j) = A^T(j)X(j+1)A(j) + C_1^T(j)C_1^T(j) - \eta_j\left(X(j+1)\right)$$

where

$$\eta_j(X(j+1)) = M_j\left(X(j+1)\right)\left(R(j) + B^T(j) \times X(j+1)B(j)\right)^{-1} M_j^T\left(X(j+1)\right)$$

and

$$M_j\left(X(j+1)\right) = A^T(j)X(j+1)B(j) + C_1^T(j)D_{1\bullet}(j).$$

Then, at the time of $j+N$, we have

$$X(j+N) = A^T(j+N)X(j+N+1)A(j+N) + C_1^T(j+N)C_1(j+N) - \eta_{j+N}\left(X(j+N+1)\right).$$

By considering that the plant $G$ in (1) is periodic with period $N$ (i.e., $A(j+N) = A(j)$, $B(j+N) = B(j)$, $C_1(j+N) = C_1(j)$, and $D_{1\bullet}(j+N) = D_{1\bullet}(j)$), we have

$$X(j+N) = A^T(j)X(j+N+1)A(j) + C_1^T(j)C_1(j) - \eta_j\left(X(j+N+1)\right) \quad (11)$$

where

$$\eta_j(X(j+N+1)) = M_j(X(j+N+1))\left(R(j) + B^T(j) \times X(j+N+1)B(j)\right)^{-1} \times M_j^T\left(X(j+N+1)\right).$$

Thus, (11) implies that $(\ldots, X(j+N), X(j+N+1), \ldots)$ is another solution to the discrete Riccati equation (6). From [10], we know that the bounded stabilizing solution to the discrete Riccati equation (6) is unique, which implies $X(j) = X(j+N)$.

As a result, all matrices $\bar{A}(k)$, $\begin{bmatrix} \bar{C}_{12}(k) \\ \bar{C}_2(k) \end{bmatrix}$, and $\begin{bmatrix} \bar{D}_{112}(k) \\ D_{21}(k) \end{bmatrix}$ for (8) are periodic with period $N$.

Moreover, the periodicity of the solution to the discrete Riccati equation (8) in Step 5, i.e., $Y(k) = Y(k+N)$, can be shown in a similar manner. Consequentially, the periodicity of $X(k)$ and $Y(k)$ implies that all of the parameters to construct the $H_\infty$ controller in (5) are periodic with period $N$. Thus, the optimal $H_\infty$ controller for the LPTV system $G$ is also periodic with period $N$. ■

The periodicity of $H_\infty$ controllers for LPTV systems provides a significant advantage, since the Riccati equations in Step 1 and Step 5 can be solved backward and forward, respectively, with zero-initial conditions by iteration and their solutions will converge to the corresponding periodic solutions.

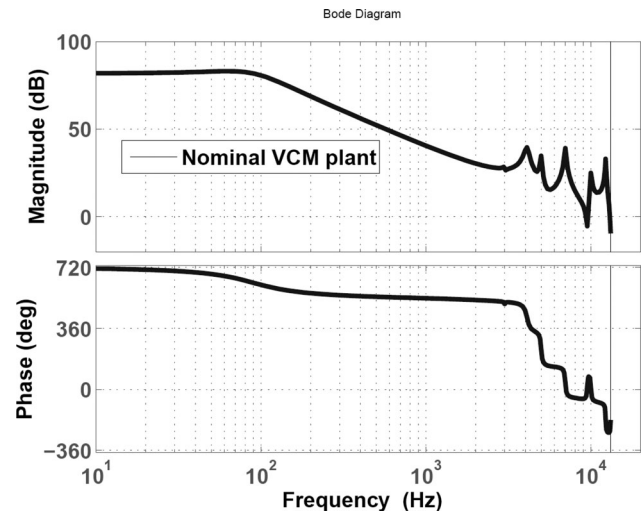


Fig. 2. HDD benchmark VCM model.

With Lemma 1, the optimal $H_\infty$ control synthesis algorithm for LPTV systems is developed as follows.

*Algorithm 1:* The following algorithm synthesizes optimal $H_\infty$ control for general LPTV systems.

1) Choose a large initial interval and a large initial value $\gamma$.
2) For a given value $\gamma$, calculate the minimum entropy controller:
   a) Solve the state-feedback Riccati equation (6) in Step 1 with zero-final conditions by iteration to obtain $X(j)\,(j = 0, \ldots, N-1)$.
   b) If $X(j) \succeq 0$ and the factorization in (7) exists for $\forall j = 0, \ldots, N-1$, continue to solve the filtering Riccati equation (8) with zero-initial conditions by iteration to obtain $Y(k)\,(k = 0, \ldots, N-1)$. Otherwise, stop.
   c) If $Y(k) \succeq 0$ and the factorization in (9) exists for $\forall k = 0, \ldots, N-1$, continue to calculate the control parameters for the minimum entropy controller. Otherwise, stop.
3) If the interval is small enough, stop. Otherwise, update the interval and $\gamma$, and then, go back to Step 2).

## IV. Design Examples for HDD Servo Systems

In order to evaluate our proposed optimal $H_\infty$ control design methodology in this paper, the algorithm will first be tested via a simulation study that utilizes a single-stage HDD benchmark model developed by the IEEJapan technical committee on Nano-Scale Servo (NSS) systems [13]. The nominal voice coil motor (VCM) model is indicated in Fig. 2. In the simulations, we will assume that the PES sampling frequency is $f_s = 26\,400$ Hz.

Notice that in this paper, we consider the real VCM plant with an output multiplicative uncertainty as

$$G_v = G_v^n(1 + W_\triangle \triangle), \qquad \|\triangle\|_\infty < 1 \quad (12)$$

where $W_\triangle$ is the plant uncertainty weighting function.

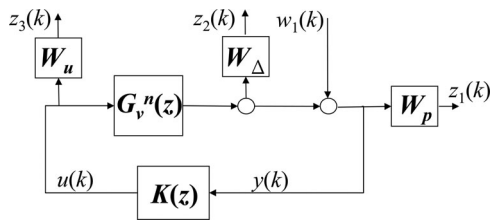


Fig. 3. Control design formulation for single-rate HDDs.

### A. Optimal $H_\infty$ Track-Following Control for Single-Rate HDD Servos

We consider the block diagram shown in Fig. 3 for the optimal $H_\infty$ control design, where $G_v^n$, $W_p$, and $W_u$ are, respectively, the nominal VCM plant, loop-shaping performance weighting function, and control input weighting value. In this example, we consider the case when the control actuation is performed at the same rate as the PES sampling rate.

Thus, it is well known that the single-rate servo system is an LTI system, which is equivalent to an LPTV system with period $N = 1$. As a result, the corresponding control problem can be equivalently stated as

$$\begin{aligned} &\min_{K,\gamma} \ \gamma \\ &\text{s.t.} \qquad \|T_{z\leftarrow w_1}\|_\infty < \gamma \ . \end{aligned} \tag{13}$$

Here, $T_{z\leftarrow w_1}$ represents the transfer function matrix from $w_1$ to $z = [\, z_1 \quad z_2 \quad z_3 \,]^T$ as shown in Fig. 3.

Notice that with $N = 1$, all of entries in the state-space realization of (1) are constant, and thus, the Riccati equation solutions in (6) and (8) converge to constant steady-state solutions that can be computed via their corresponding discrete algebraic Riccati equations (DAREs). Consequentially, the synthesized optimal $H_\infty$ controllers for LTI systems are also time invariant.

In order to investigate the accuracy of the control synthesis algorithm presented in this paper, we compare a controller that is synthesized by Algorithm 1 to the one that is synthesized by the MATLAB function of "hinfsyn" in the Robust Control Toolbox using identical plant parameters and weighting functions. Notice that the "hinfsyn" function in the MATLAB version of R2007b performs $H_\infty$ control synthesis for discrete-time systems by first mapping the discrete-time plant to a continuous-time plant using the bilinear transformation, performing $H_\infty$ control synthesis in the continuous-time domain and, then, mapping the resulting $H_\infty$ continuous-time control back to the discrete-time domain using the bilinear transformation.

For the comparison, the weighting functions $W_p$ and $W_\triangle$ and the weighting value $W_u$ are selected so that the developed $H_\infty$ control synthesis technique yields a solution to the minimization problem in (13) with $\gamma \leq 1$. In this paper, the continuous-time uncertainty weighting function is chosen as

$$W_\triangle(s) = \frac{0.11s + 767.8}{s + 9598} \ . \tag{14}$$

In this section, $W_u = 2 \times 10^{-5}$ was selected so that the achieved $\gamma$ is less than or equal to 1, and simultaneously, the control actuation generated by the resulting controller is appropriate under the hardware constraints of real HDD servo systems.

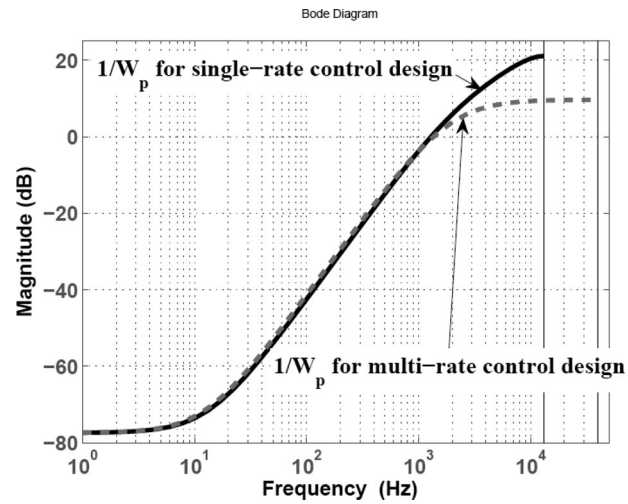


Fig. 4. Magnitude Bode plots of performance weighting functions.

For the single-rate design, the magnitude Bode plot of the performance weighting function inverse is illustrated in Fig. 4. With $\gamma \leq 1$, the designed servo is able to achieve the robust performance that the magnitude Bode plot of the designed error-rejection transfer function is below that of $|W_p(\omega)|^{-1}$ for all uncertainties characterized by the uncertainty weighting function $W_\triangle$ in (14).

The design results are illustrated in Fig. 5, which shows the magnitude Bode plot of the closed-loop error-rejection transfer functions when the $H_\infty$ controller is synthesized using the methodology proposed in this paper and when it is synthesized using the MATLAB function "hinfsyn." As shown in the figure, the MATLAB function "hinfsyn" failed to synthesize a controller that could achieve the specified robust performance, while the synthesis technique proposed in this paper produced an optimal $H_\infty$ controller that satisfied all constraints with a minimum $\gamma^* = 0.99$. As stated in [9], the successive uses of the bilinear transformation (discrete time to continuous time and, then, back to discrete time) in the MATLAB function "hinfsyn" may introduce numeric accuracy problems, particularly, when the systems are ill conditioned.

### B. Optimal $H_\infty$ Track-Following Control for Multirate HDD Servos

In this section, the effectiveness of the developed control synthesis algorithm will be evaluated by designing optimal $H_\infty$ track-following controllers for multirate HDD servos. As discussed in [14], [15], increasing the control actuation rate can improve both track-following control performance and robustness. In this section, we validate this idea by comparing the single-rate $H_\infty$ controller that was designed in the previous section to a multirate $H_\infty$ controller, where the actuation rate $f_a$ is three times higher than the PES sampling rate $f_s$. In addition, since the higher rate actuation can be exploited to improve the control performance, a more aggressive performance weighting

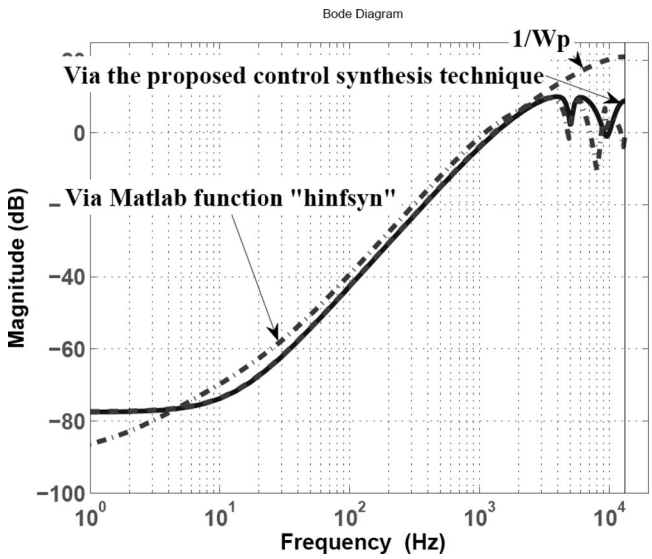


Fig. 5. Sensitivity functions for the single-rate HDD servo.

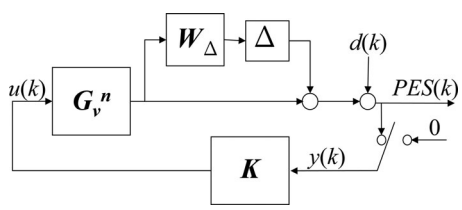


Fig. 6. HDD servo system with unavailable PES samples.

function, shown in Fig. 4, has been utilized for the multirate control design. Because of the higher actuation rate, it is necessary to discretize the plant model and the weighting functions indicated in Fig. 3 at the actuation rate $f_a$, i.e. at the faster rate. We, then, assume that PES measurements are only available at the instances $k \in \{0, N, 2N, \ldots\}$ where $N = 3$. Thus, HDD servo control systems with multirate sampling and actuation can be modeled by the block diagram shown in Fig. 6.

Here, $d$ is the overall contribution of all disturbances [16] including torque disturbance, windage, nonrepeatable disk motions, and measurement noise to PES. For the optimal $H_\infty$ control of such a multirate HDD servo system, we are also interesting in designing a controller $K$ satisfying the following conditions:

$$\|T_s \cdot W_p\|_{2\leftarrow 2} < 1 \quad \forall \|\triangle\|_\infty \leq 1 \tag{15}$$

where $T_s$ is the sensitivity function (i.e., error-rejection transfer function) from $d$ to PES, as shown in Fig. 6, while $W_p$ is the loop-shaping performance weighting function.

From the standard assumption for the optimal $H_\infty$ control [12], the derived controller requires a condition $D_{21}(k)D_{21}^T(k) \succ 0$ for all $k$. Unfortunately, the typical approach to enforce multirate sampling and actuation [14] will not work here because this would result in $D_{21}(k)D_{21}^T(k)$ being singular. In this paper, we consider the block diagram shown in Fig. 7 for the multirate optimal $H_\infty$ control synthesis. Here, we introduce a fictitious disturbance input $w_2$, which will be

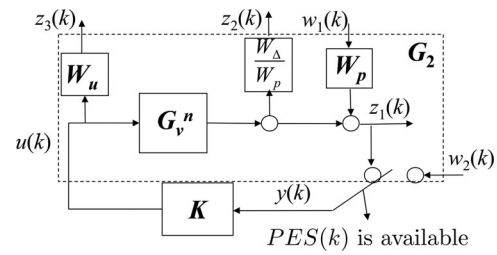


Fig. 7. Control design formulation for HDDs with multirate sampling and actuation.

injected into the feedback signal $y$ when the PES is unavailable so that the nonsingularity assumption of $D_{21}(k)D_{21}^T(k)$ can be attained. Notice that if the gain of the resulting time-varying controller $K$ is zero when the PES measurement is unavailable at the time of $k$, then this fictitious noise will not affect the minimum closed-loop-induced norm and the resulting optimal $H_\infty$ controller. This expectation is achieved when the minimum entropy $H_\infty$ control synthesis technique proposed in this paper is used, as will be discussed in detail later.

Unlike the standard $H_\infty$ control problem formulation [17], the performance weighting function here is moved to the disturbance input side. By doing so, the feedback signal $y$ is affected by a "colored" disturbance $W_p w_1$ more directly when the sampling rate is lower than the actuation rate. In order to maintain the same $H_\infty$ constraints as those that were used in Section IV-A, it is necessary to use the control-synthesis architecture shown in Fig. 7, where the weighting functions $W_p$ and $W_\triangle$ are the same as the weighting functions in Section IV-A.

As a result, we can formulate the optimal $H_\infty$ control design problem in (4) by replacing the system $G$ by $G_2$, where $G_2$ is indicated by the dashed box in Fig. 7. Thus, $G_2$ is the open-loop map from $[\,w_1 \quad w_2 \quad u\,]^T$ to $[\,z_1 \quad z_2 \quad z_3 \quad y\,]^T$, which can be represented by the following LPTV system with period $N = 3$:

$$G_2 \sim \begin{bmatrix} x(k+1) \\ z(k) \\ y(k) \end{bmatrix} = \begin{bmatrix} A & B_1 & B_2 \\ C_1 & D_{11} & D_{12} \\ C_2(k) & D_{21}(k) & 0 \end{bmatrix} \begin{bmatrix} x(k) \\ w(k) \\ u(k) \end{bmatrix} \tag{16}$$

where

$$[\,C_2(k) \quad D_{21}(k)\,] = \begin{cases} [\,C_{2m} \quad [\,D_{21m} \quad 0\,]\,], & \text{PES is unavailable} \\ [\,0 \quad [\,0 \quad 1\,]\,], & \text{otherwise.} \end{cases} \tag{17}$$

Notice that all the matrices (16) are constants except $C_2(k)$ and $D_{21}(k)$. Since all the matrices involved in the computation of the state-feedback Riccati equation solution (6) in Step 1 are constant, the solution $X(k)$ will converge to a constant matrix, which can be computed via its corresponding DARE. Moreover, the parameters $X$, $T$, and $F$ that are computed in Steps 1–3 are constant, which implies that the parameters $\bar{A}(k)$ and $T_{22}^{-1}(k)\bar{C}_{12}(k)$ in the proposed controller (5) will also be constant. Additionally, the filtering Riccati equation solution $Y(k)$, which is computed forward in time using (8) and a zero-initial

TABLE I
SIMULATION RESULTS FOR SINGLE- AND MULTIRATE CONTROL DESIGNS

| | $3\sigma$ PES (% of track) | |
|---|---|---|
| | Nominal | Worst |
| Single-rate design | 10.7 | 11.4 |
| Multi-rate design | 9.2 | 9.6 |

condition, will converge to a steady-state periodic solution with period $N$, as demonstrated in Lemma 1. It turns out that the filter gains $F_t(k)$ and $L_t(k)$ will also be periodic with period $N$. It can also be shown [12] that both $\tilde{T}_{12}(k)$ and $\tilde{F}_2(k)$ are equal to zero at the instance $k$ when the PES is unavailable. Thus, both $F_t(k)$ and $L_t(k)$ are also equal to zero at these instances, justifying the use of the fictitious disturbance $w_2$ in the control synthesis methodology. As a result, the minimum closed-loop $\ell_2$-induced norm and the optimal $H_\infty$ controller are unaffected by the use of the fictitious disturbance $w_2$ in the control synthesis. With the zero gains of $F_t(k)$ and $L_t(k)$ at the instance when the PES is unavailable, the time-varying control parameter $\bar{C}_2(k) = C_2(k) + D_{21}(k)F_1$ in (5) can be simply replaced by the constant parameter $\bar{C}_{2m} = C_{2m} + [\, D_{21m} \quad 0\,]F_1$ without changing the controller. As a result, for the HDD servo systems with multirate sampling and actuation, all of the control parameters of the minimum entropy $H_\infty$ controller shown in (5) are constant except $F_t(k)$ and $L_t(k)$.

Performing a multirate optimal $H_\infty$ control synthesis described earlier produces a multirate $H_\infty$ controller that returns the minimum $\ell_2$-induced norm of $\gamma^* = 1$.

With the more aggressive performance weighting function shown in Fig. 4, the obtained optimal $\ell_2$-induced norm of $\gamma^* = 1$ implies that the multirate strategy has the ability to improve the control performance. In order to further highlight the performance and robustness improvement that can be attained by the presented control synthesis algorithm for a higher actuation rate, a time-domain simulation study was performed using both the single-rate optimal $H_\infty$ control designed in Section IV-A and the multirate optimal $H_\infty$ control designed in this section. To evaluate the robust performance of the two control designs, each controller was tested on 50 different plants, which were randomly generated from (12) with the uncertainty weighting function in (14) by using MATLAB function "`usample`." Note that the disturbance models for our time-domain simulation are provided in [13].

Table I contains the root-mean-square $3\sigma$ values of the PES for the nominal plant and the worst-case results for each controller. These results indicate that a controller with a higher actuation rate is able to not only reduce the $3\sigma$ PES by $14.0\%$ for the nominal plant, but also improve the servo performance for the worst-case situation by $15.8\%$.

## V. EXPERIMENTAL STUDY

In order to further evaluate our proposed optimal $H_\infty$ control synthesis methodology, we used the proposed algorithm to design a controller and, then, implemented the resulting controller on a real HDD with missing PES samples. The tested HDD was provided by Western Digital Corporation. For this $3.5''$ disk drive, the number of servo sectors is $256$ and the spindle rotation speed is 7200 r/min. The servo patterns on some servo sectors at the inside diameter (ID) are unaccessible for the servo system to generate the PES. Specifically, we found that the PES is unavailable in the following 51 servo sectors:

$M_{\text{miss}} = \{0, 4, 8, 17, 21, 25, 34, 38, 42, 47, 51, 55, 59, 64, 68, 72, 81, 85, 89, 98, 102, 106, 111, 115, 119, 123, 128, 132, 136, 145, 149, 153, 162, 166, 170, 179, 183, 187, 192, 196, 200, 209, 213, 217, 226, 230, 234, 239, 243, 247, 251\}$.

Such an HDD servo with missing PES samples can be still represented as the block diagram in Fig. 6 and we also consider the block diagram shown in Fig. 7 for the optimal $H_\infty$ control synthesis [2]. Then, the system shown in (16) has a large period, i.e., $N = 256$.

As presented in [2], the nominal VCM model $G_v^n(s)$ was identified to match the experiment frequency response, which was measured on the disk area, where there are no missing PES samples. Note that in order to reduce the control order, the nominal VCM plant was identified as an eighth-order model. In addition, the weighting functions for the control design formulation in Fig. 7 were determined as

$$W_\triangle(z) = \frac{0.985z - 0.693}{z + 0.041}$$

$$W_p(z) = \frac{0.156z^5 - 0.666z^4 + 1.14z^3 - 0.968z^2 + 0.41z - 0.07}{z^5 - 4.933z^4 + 9.739z^3 - 9.617z^2 + 4.75z - 0.939}$$

$$W_u = 4.$$

As a result, the VCM plant could have an unstructured uncertainty producing the $\pm 28\%$ gain variation at low frequency and the $\pm 175\%$ gain variation at high frequency with the chosen $W_\triangle$, while the frequency response of $W_p^{-1}$ associated with disturbance attenuation is shown in Fig. 9.

After applying our developed control algorithm, an optimal $\ell_2$-induced norm of $\gamma^* = 0.91$ was obtained. We used balanced truncation [18] to reduce the order of the resulting controller from 19 to 12. This allowed us to implement the controller on the disk drive's own processor by changing the firmware code. In addition, since the control parameters $F_t(k)$ and $L_t(k)$ in (5) are time varying, we have to reduce the number of these control parameters for their implementation on real HDDs. As demonstrated in [2], the nonzero time-varying parameters $F_t(k)$ and $L_t(k)$ have very small variations, which motivates us to approximate these time-varying control parameter values using their average values over $M_{\text{miss}}$. Finally, the controller was simplified as

$$\begin{cases} \begin{bmatrix} \hat{x}_{2i-1}(k+1) \\ \hat{x}_{2i}(k+1) \end{bmatrix} = \begin{bmatrix} 0 & a_{2i-1} \\ 1 & a_{2i} \end{bmatrix} \begin{bmatrix} \hat{x}_{2i-1}(k) \\ \hat{x}_{2i}(k) \end{bmatrix} \\ \quad + \begin{bmatrix} f_{2i-1}(k) \\ f_{2i}(k) \end{bmatrix} \tilde{y}(k) + \begin{bmatrix} 1 \\ 0 \end{bmatrix} u(k), \quad i = 1, \ldots, 5 \\ \hat{x}_j(k+1) = a_j \hat{x}_j(k) + u(k), \qquad j = 11, 12 \\ \tilde{y}(k) = \sum_{i=1}^{12} c_i \hat{x}_i(k) - y(k) \\ u(k) = \sum_{i=1}^{12} m_i \hat{x}_i(k) - D_t(k)\tilde{y}(k) \end{cases} \tag{18}$$

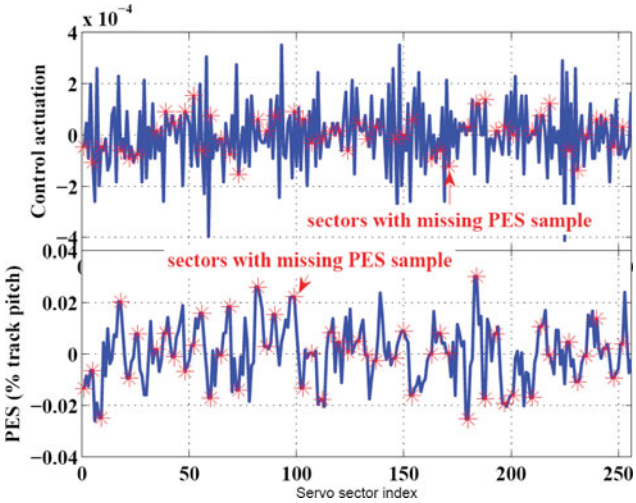


Fig. 8. Control signal and PES in the time domain.

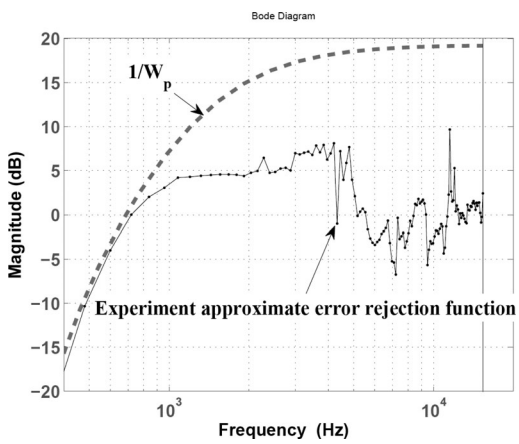


Fig. 9. Experiment result for the experimental approximate error-rejection function.

where

$$\{f_1(k), \ldots, f_{12}(k), D_t(k)\} = \begin{cases} \{f_{1,s}, \ldots, f_{12,s}, D_{t,s}\}, & k \in M_{\text{miss}} \\ \{0, \ldots, 0, 0\}, & \text{otherwise.} \end{cases}$$

The time-domain control signal and PES for one revolution are shown in Fig. 8, where the servo sector with a missing PES sample is marked by "*". In the plot, when a missing PES sample occurs, the unavailable PES is approximated by the previous available one. However, the control signal is always updated using (18) even when the PES is unavailable. Fig. 9 shows the magnitude frequency responses of $W_p^{-1}$ and the measured approximate error-rejection function [2]. Since the achieved optimal $\ell_2$-induced norm is less than 1, the measured approximate error-rejection function should be below the inverse of the performance weighting function at every frequency, which is verified by the experimental result shown in Fig. 9. Thus, the experimental result demonstrates the effectiveness of our proposed control synthesis algorithm in handling a large period ($N = 256$) for HDDs with missing PES samples. Moreover, the experimental result confirms that the optimal $H_\infty$ controller synthesized by our proposed control algorithm achieved the desired disturbance attenuation.

## VI. Conclusion

The optimal $H_\infty$ control synthesis via discrete Riccati equations for general discrete-time LPTV systems was studied in this paper. Using the results in [10], we first developed the optimal $H_\infty$ control synthesis algorithm for general discrete-time LTV systems. The control synthesis algorithm was subsequently applied to LPTV systems, and it was verified that the resulting controllers are also periodically time varying. The presented control synthesis technique was evaluated by designing both single-rate and multirate optimal $H_\infty$ track-following controllers for HDDs. In the case of single-rate control, the optimal $H_\infty$ controller designed using the proposed synthesis technique was compared to the one designed using the MATLAB function 'hinfsyn." Simulation results suggested that the former technique is more numerically robust in calculating optimal discrete-time $H_\infty$ controllers for discrete-time LTI systems than the latter. Simulation results further demonstrated that the presented control synthesis algorithm is also applicable to HDD servos with multirate sampling and actuation, while the "hinfsyn" function in MATLAB is only applicable for LTI plants. Moreover, an experimental study, which consisted of implementing the developed control algorithm on a real disk drive with missing PES sampling data, demonstrated its effectiveness in handling LPTV systems with a large period and attaining desirable disturbance attenuation.

## Acknowledgment

The authors would like to thank Western Digital Corporation, Irvine, CA, for providing invaluable information to perform this study.

## References

[1] M. Gei, S. Roccabianca, and M. Bacca, "Controlling bandgap in electroactive polymer-based structures," *IEEE/ASME Trans. Mechatronics*, vol. 16, no. 1, Feb. 2011.

[2] J. Nie, E. Sheh, and R. Horowitz, "Optimal $H_\infty$ control for hard disk drives with an irregular sampling rate," presented at the Amer. Control Conf., 2011, San Francisco, CA.

[3] R. Conway and R. Horowitz, "Guaranteed cost control for linear periodically time-varying systems with structured uncertainty and a generalized $H_2$ objective," *Mechatronics*, vol. 20, no. 1, pp. 12–19, 2010.

[4] K. Kalyanam and T. Tsao, "Experimental study of adaptive-Q control for disk drive track-following servo problem," *IEEE/ASME Trans. Mechatronics*, vol. 15, no. 3, pp. 480–491, Jun. 2010.

[5] K. Chan, W. Liao, and I. Shen, "Precision positioning of hard disk drives using piezoelectric actuators with passive damping," *IEEE/ASME Trans. Mechatron.*, vol. 13, no. 1, pp. 147–151, Feb. 2008.

[6] A. Iqbal, Z. Wu, and F. Ben Amara, "Mixed-sensitivity $H_\infty$ control of magnetic-fluid-deformable mirrors," *IEEE/ASME Trans. Mechatronics*, vol. 15, no. 4, pp. 548–556, Aug. 2010.

[7] G. Zames, "Feedback and optimal sensitivity: Model reference transformations multiplicative seminorms, and approximate inverses," *IEEE Trans. Autom. Control*, vol. 26, no. 2, pp. 301–320, Apr. 1981.

[8] J. Doyle, K. Glover, P. Khargonekar, and B. Francis, "State-space solutions to standard $H_2$ and $H_\infty$ control problems," *IEEE Trans. Autom. Control*, vol. 34, no. 8, pp. 831–847, Aug. 1989.

[9] P. Iglesias and K. Glover, "State-space approach to discrete-time control," *Int. J. Control*, vol. 54, no. 5, pp. 1031–1073, 1991.

[10] M. A. Peters and P. A. Iglesias, *Minimum Entropy Control for Time-Varying Systems. Systems and Control: Foundations and Applications*. Boston, MA: Birkhäuser, 1997.
[11] R. Conway and R. Horowitz, "Analysis of $H_2$ guaranteed cost performance," presented at the Dyn. Syst. Control Conf., Hollywood, CA, 2009.
[12] J. Nie, "Control design and implementation of hard disk drives," Ph.D. dissertation, Dept. Mech. Eng., Univ. California, Berkeley, 2011.
[13] IEEJapan technical committee on Nano-Scale Servo (NSS) system. (2006). [Online]. Available: http://mizugaki.iis.u-tokyo.ac.jp/nss/
[14] R. Nagamune, X. Huang, and R. Horowitz, "Multi-rate track-following control with robust stability for a dual-stage multi-sensing servo systems in HDDs," in *Proc. Joint 44th IEEE Conf. Decision Control Eur. Control Conf.*, 2005, pp. 3886–3891.
[15] L. Yang and M. Tomizuka, "Short seeking by multirate digital controllers for computation saving with initial value adjustment," *IEEE/ASME Trans. Mechatronics*, vol. 11, no. 1, pp. 9–16, Feb. 2006.
[16] J. Nie and R. Horowitz, "Design and implementation of dual-stage track-following control for hard disk drives," presented at the Dyn. Syst. Control Conf., Hollywood, CA, 2009.
[17] S. Skogestad and I. Postlethwaite, *Multivariable Feedback Control: Analysis and Design*. Hoboken, NJ: Wiley, 2005.
[18] B. Moore, "Principal component analysis in linear systems: Controllability, observability, and model reduction," *IEEE Trans. Autom. Control*, vol. 26, no. 1, pp. 17–31, Feb. 1981.

**Jianbin Nie** received the B.S. degree in automation from the University of Science and Technology of China, Hefei, China, in 2006, and the Ph.D. degree in mechanical engineering from the University of California, Berkeley, in 2011.

Currently, he is with Western Digital Corporation, Irvine, CA. His research interests include control design and implementation of dual-stage hard disk drive servos, concentric self-servo track-writing servos, and track-following servos with irregular sampling rates.

**Richard Conway** (S'09) received the B.S., M.S., and Ph.D. degrees in mechanical engineering from the University of California, Berkeley (UC Berkeley), in 2004, 2008, and 2011, respectively.

Currently, he is a Postdoctoral Researcher in the Department of Mechanical Engineering at UC Berkeley. His research interests include optimal robust performance control, algorithms for system analysis and controller synthesis, Riccati equations in control, convex optimization in control, periodic discrete-time systems, identification of parametrically uncertain systems, and model reduction.

Dr. Conway is a student member of the American Society of Mechanical Engineers.

**Roberto Horowitz** (SM'89) received the B.S. degree (Hons.) in 1978 and the Ph.D. degree in mechanical engineering in 1983 from the University of California, Berkeley.

In 1982 he joined the Department of Mechanical Engineering, University of California, Berkeley, where he is currently a Professor and the James Fife Endowed Chair. His research interests include the areas of adaptive, learning, nonlinear and optimal control, with applications to microelectromechanical systems (MEMS), computer disk file systems, robotics, mechatronics, and intelligent vehicle and highway systems (IVHS).

Dr. Horowitz is a senior member of the American Society of Mechanical Engineers.